

# **Bond Performance of GFRP Bars Embedded into Low Carbon Concrete and Portland Cement Blocks**

**Manjola Caro<sup>1</sup>, Victor Wiles<sup>2</sup>, Matthias Nahum<sup>2</sup>**

<sup>1</sup>University of Bristol

Queens Building, University Walk, Bristol, UK, BS8 1TR  
manjola.caro@bristol.ac.uk; jn21549@bristol.ac.uk

<sup>2</sup>University of Bristol

Queens Building, University Walk, Bristol, UK, BS8 1TR  
fa20893@bristol.ac.uk

**Abstract** - Retrofitting of strength-deficient reinforced concrete (RC) infrastructure assets, in particular bridges, is an issue of global significance. In the context of sustainable development and climate change mitigation, demand for alternative low carbon building materials that can reduce the construction sector's large carbon footprint is increasing. The integration of fibre-reinforced polymer (FRP) materials to RC structures has become a prevalent sustainable alternative due to their high strength-to-weight ratio and durability, corrosion resistance and enhancement of shear capacity. The deep embedment (DE) technique is a superior technique for concrete shear strengthening. In this method, vertical holes are drilled upwards from the soffit in the shear spans of existing concrete beams. High viscosity epoxy resin is then injected into the drilled holes and steel or FRP bars are embedded into the concrete core. This study investigates, for the first time, the bond performance of deep embedment (DE) glass fibre reinforced polymer (GFRP) bars epoxy-bonded into a new type of low carbon, alkali-activated concrete (AAC) which is tested against Ordinary Portland cement (OPC). The experimentally investigated parameters include the concrete type, concrete compressive strength, GFRP bar diameter and hole diameter. The results show that the pull-out capacity increased with the increase in bar diameter and concrete compressive strength. The increase in hole diameter affected both the initial stiffness and failure loads of the specimens with DE GFRP bars. The results suggest that adopting a hole diameter of  $1.5d_b$  enhances the bond behaviour of the DE technique. The specimens with low carbon, AAC achieved higher pull-out capacities and better bond performance than the corresponding specimens with OPC, making AAC an eco-friendly alternative to enhancing the sustainability of large-scale construction without compromising the efficiency of the DE technique.

**Keywords:** glass fibre reinforced polymer (GFRP), low carbon, alkali-activated concrete, pull-out test, bond strength, epoxy resin, deep embedment (DE) technique.

## **1. Introduction**

Climate change is an ever-increasing issue and the preventative measures that must be taken as an industry to mitigate its affects are more important than ever. Concrete is an essential part of modern-day infrastructure as it is the most used structural material in the construction industry. With its vast variety of uses and thus demand, comes the need for reparations and replacements over its extended design life. This leads to needing alternative low carbon solutions to reducing the construction sector's large carbon footprint [1].

Rehabilitating of strength-deficient reinforced concrete (RC) structures which are susceptible to shear brittle failure can be done in a multitude of ways. Fibre-reinforced polymer (FRP) shear-strengthening techniques such as near-surface mounted (NSM) bars and externally bonded (EB) sheets/plates have been proven effective in improving the shear capacity [2]. However, they are limited in situations where all faces of the beam are not accessible or if they are poorly anchored to the concrete, causing the systems to debond prematurely [2].

The deep embedment (DE) technique is a superior advancement in the shear strengthening of RC structures. In this technique, vertical or inclined holes are drilled upwards from the soffit in the shear spans of RC beams and high viscosity epoxy is injected into the drilled holes to bond FRP or steel bars to the concrete core through a full-depth connection [3,4]. The DE method provides higher strengthening effectiveness because, unlike the externally bonded (EB) and near-surface mounted (NSM) techniques, in the DE method the concrete core transfers the stresses to the bars. Therefore, the DE technique prevents the debonding and de-lamination of concrete cover failure mechanisms [4]. Previous experimental results reported

a shear strength increase of 61%, 31% and 23% for DE carbon-FRP (CFRP) bars, NSM CFRP rods and EB CFRP sheets, respectively [2].

Pull-out tests have been adopted by researchers as a practical approach to examining the bond performance for both FRP and steel bars epoxy-bonded in traditional OPC blocks [3,4,5]. Experimental results have reported that the bond between the DE bar and the concrete core plays a major role in the shear-strengthening effectiveness of the DE technique. It has been shown that an adequate amount of high-strength and high-viscosity epoxy adhesive is needed to prevent debonding failure and achieve a better bond contact between the concrete and DE bar [3]. In addition, it has been found that DE FRP bars with plain surfaces provided a higher shear strength enhancement than sand-coated bars due to a better shear transfer along the bar–epoxy interface [4].

Other key parameters that influence the DE bar-concrete bond behaviour include the embedment length, concrete strength, DE bar diameter and hole diameter. It has been reported that for all DE bar types as the embedded length increased, the average bond stress decreased [3,4,5]. Whereas, as concrete strength increased, the maximum average bond stress also increased. Studies have shown that increasing the concrete compressive strength increases the resistance of the DE bar–concrete interface, which enhances the bond strength [4,5,6]. Experimental results have shown that the bond capacity is higher for FRP bars of greater diameter due to a larger contact area, resulting in a higher bond force [4,5].

The FRP bar type also affected the DE bond performance. DE systems with steel and carbon-FRP bars which have an elastic modulus considerably higher than that of aramid-FRP and glass-FRP bars managed to achieve a better bond performance and a more ductile bond stress-slip response [3]. The effect of quantity of adhesive (i.e. hole diameter) also affected the bond behaviour. It has been recommended using an optimum hole diameter of about 1.5 times that of the bar diameter ( $1.5d_b$ ) [4].

However, the bond behaviour of DE FRP bars epoxy-bonded into low carbon, alkali-activated concrete (AAC) has not been previously examined. This research study examines, for the first time, the bond performance of DE GFRP bars epoxy-bonded into a new type of AAC which is tested against Ordinary Portland cement (OPC). Cemfree Optima™, a one-part alkali-activated cement primarily composed of Ground Granulated Blast Furnace Slag (GGBS) which can be mixed with aggregate and water directly in the presence of a liquid alkali activator was used. It has been reported that replacing 100% of the OPC with a Cemfree binder leads to a reduction of embodied CO<sub>2</sub> of up to 80% in comparison to the OPC-based concrete without compromising the durability and shear strength [1]. Therefore, the results will enable understanding of the FRP-to-AAC interfacial bond behaviour which is crucial to the safe implementation of the DE technique. These results will also demonstrate the benefits in adopting eco-friendly concrete with minimal carbon emissions and innovative FRP composite materials for the shear strengthening of concrete structures. Hence, the benefits of this research study are in line with the net zero targets policy imposed by various companies in the construction industry [1].

The objectives of this research study are:

- a) To investigate the bond behaviour of the DE GFRP bars epoxy-bonded into 100 mm × 100 mm × 100 mm cubes of AAC as well as OPC.
- b) To carry out a comprehensive assessment of the effect of concrete type, concrete strength, bar diameter and hole diameter on the bond behaviour.

## 2. Experimental Programme

The experimental programme is conducted in line with the ACI 440.1R-06 guidelines [7] and previously experimental pull-out test studies on the DE technique [3,4,5]. A total of eighteen concrete cube specimens with embedded GFRP bars using an epoxy adhesive were tested as reported in Table 1. A pull-out load was applied on the GFRP bars in order to obtain the average bond-slip relationships at the loaded end of the tested bars.

The experimentally investigated parameters were the concrete type, concrete compressive strength, GFRP bar diameter and hole diameter. The following sections provide a description of the material properties, test specimens, installation of FRP bars and the pull-out test setup for this study.

## 2.1. Materials

Three batches of concrete were cast. Two concrete mixes were designed according to the BRE guidelines [8]. Portland cement (class C20/25 and C25/30) and aggregates with a maximum size of 10 mm were used in OPC concrete batches. For the other remaining batch Cemfree Optima™ ultra binder was used, which contained 95% GGBS, and 5% Cemfree activator. The Cemfree ultra binder was used as a low carbon alternative to the C20/25 OPC specimens. All specimens used aggregates with a maximum size of 10 mm. The intended water to binder ratio (w/b ratio) was 0.37 for the low carbon, AAC specimens and 0.5 and 0.46 for the C20/25 and C25/30 specimens, respectively.

Each concrete batch was used to cast between four to eight pull-out concrete cubes (100 mm × 100 mm × 100 mm) and six ancillary control samples (three cubes (100 mm × 100 mm × 100 mm) and three cylinders (100 mm diameter × 200 mm height)). The control specimens were used to estimate the concrete compressive strength. The average measured cylinder compressive strengths on the day of pull-out testing were 21.6 MPa (referred to as C22), 26.5 MPa (referred to as C27) for the OPC mixes and 21.5 MPa (referred to as LC22) for the low carbon, AAC mix.

One type of GFRP bar (unidirectional E-glass roving) with smooth polyester matrix finish was used. Two diameters of GFRP bars were assessed in this study, 10 mm and 12 mm. The GFRP bars had an elastic modulus, tensile strength and ultimate strain of 27 GPa, 500 MPa and 1.64%, respectively, as tested by the manufacturer.

A commercially available high viscosity epoxy resin (Araldite 2019) was used to bond the DE GFRP bars to AAC and OPC blocks. This epoxy resin had a compressive strength, compressive modulus, tensile strength, bond strength and ultimate strain at failure of 65 MPa, 1500 MPa, 40 MPa, 36 MPa and 4.3%, respectively, as certified by the manufacturer.

## 2.2. Test Specimens

Table 1 provides a summary of the pull-out test specimens and test results. Each specimen is characterised by a four-part designation. The first part (either LC22, C22 or C27) specifies the concrete type and cylinder compressive strength. The second part specifies the FRP bar type and diameter (GFRP 10/12). The third part identifies the embedded length of the FRP bar ( $5d_b$ , where  $d_b$  is the nominal bar diameter). The last part represents the hole diameter (either  $1.25d_b$ ,  $1.5d_b$  or  $1.8d_b$ ). Hence LC22-GFRP10- $5d_b$ - $1.25d_b$  refers to a specimen of low carbon, AAC with a cylinder compressive strength of 21.5 MPa, 10 mm diameter GFRP bar, embedment length of  $5d_b$  (50 mm) and a central hole with a diameter of  $1.25d_b$  (12.5 mm).

Three sets of specimens were repeated twice to examine repeatability of test results. These were chosen to cover all concrete types over a range of central values, ensuring greater accuracy in comparison between key results.

## 2.3. Installation of GFRP bars

In order to install the GFRP bars, vertical holes were cast along the centreline of the 100 mm concrete cubes using polyvinyl chloride (PVC) rods with diameters ( $d$ ) of either 12.5mm, 15mm, 18mm and 22mm ( $d = \text{epoxy thickness} + d_b$ ).

Specialist 3D printed clamps were attached to the edges of the moulds (Fig. 1a), to ensure the PVC rod was held vertically during casting and initial curing. The clamps and rods were positioned prior to the casting, and a thin layer of release agent was brushed over the PVC rods and the five faces in contact with the moulds to ease the removal of PVC rods. PVC tape (Fig. 1b) was used to control the embedded length of the GFRP bars in the pull-out specimens to the desired length ( $5d_b$ ).

De-moulding of all the concrete specimens and the removal of the PVC rods were carried out 24 hours after casting. Following de-moulding, specimens were left to cure in a water tank at a temperature measured to be 12°C for 28 days after which they were dried for a further 24 hours before being cleaned with compressed air.

Before installing the GFRP bars, a wire brush was used to roughen the internal walls of the holes and compressed air was applied to clean the holes from any residues. The bottom ends of the holes were blocked to prevent leakage and high viscosity (Araldite 2019) was injected to fill two-thirds of the holes. A thin layer of epoxy was also applied along the embedded length of the FRP bars. The bars were then twisted as being inserted into the holes in a vertical position to ensure that no air pockets were formed inside the hole. The excess epoxy was removed from the top surface of the hole and the specimens were then cured for a week before pull-out testing.

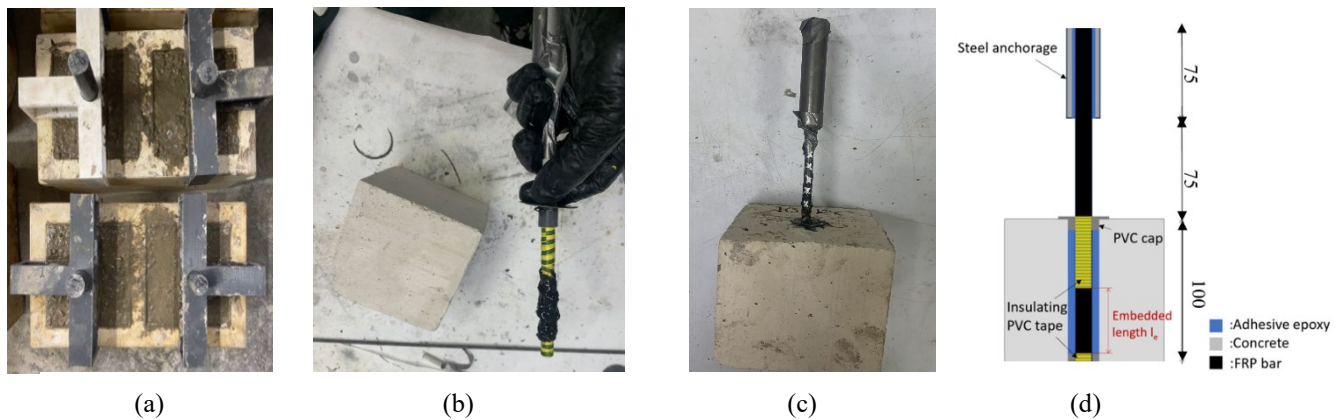


Fig. 1: Installation of GFRP bars: (a) casting, (b) prior to installation, (c) once installed, (d) diagram.

Table 1: Test specimens and test results.

Specimen ID	Peak pull-out force (kN)	Maximum average bond stress (MPa)	Slip at peak pull-out force (mm)	Failure mode
LC 22- GFRP10-5d <sub>b</sub> -1.25d <sub>b</sub>	13.51	8.60	4.05	Bar pull-out
LC 22- GFRP10-5d <sub>b</sub> -1.5d <sub>b</sub>	4.47	2.84	1.62	Bar pull-out
LC 22- GFRP10-5d <sub>b</sub> -1.5d <sub>b</sub>	5.53	3.52	2.48	Bar pull-out
LC 22- GFRP10-5d <sub>b</sub> -1.8d <sub>b</sub>	15.73	10.01	4.26	Bar pull-out
LC 22- GFRP10-5d <sub>b</sub> -1.8d <sub>b</sub>	13.69	8.72	4.08	Bar pull-out
LC 22- GFRP12-5d <sub>b</sub> -1.5d <sub>b</sub>	8.99	3.97	2.81	Bar pull-out
LC 22- GFRP12-5d <sub>b</sub> -1.5d <sub>b</sub>	5.08	2.25	1.05	Bar pull-out
LC 22- GFRP12-5d <sub>b</sub> -1.8d <sub>b</sub>	4.21	1.86	0.31	Bar pull-out
C22- GFRP10-5d <sub>b</sub> -1.25d <sub>b</sub>	6.64	4.23	2.47	Bar pull-out
C22- GFRP10-5d <sub>b</sub> -1.5d <sub>b</sub>	3.33	2.12	0.77	Bar pull-out
C22- GFRP10-5d <sub>b</sub> -1.5d <sub>b</sub>	7.45	4.74	2.33	Bar pull-out
C22- GFRP10-5d <sub>b</sub> -1.8d <sub>b</sub>	5.97	3.78	1.41	Bar pull-out
C22- GFRP12-5d <sub>b</sub> -1.5d <sub>b</sub>	9.05	4.01	2.72	Bar pull-out
C22- GFRP12-5d <sub>b</sub> -1.5d <sub>b</sub>	5.36	2.37	1.87	Bar pull-out
C27- GFRP10-5d <sub>b</sub> 1.25d <sub>b</sub>	11.87	7.56	2.78	Bar pull-out
C27- GFRP10-5d <sub>b</sub> -1.5d <sub>b</sub>	13.10	8.34	3.82	Bar pull-out
C27- GFRP10-5d <sub>b</sub> -1.8d <sub>b</sub>	13.81	8.79	2.66	Bar pull-out
C27- GFRP12-5d <sub>b</sub> -1.8d <sub>b</sub>	15.05	6.66	4.42	Bar pull-out

## 2.4. Test Setup

Figure 1 illustrates the pull-out test setup. The test procedure for the pull-out test followed the ACI 440.1R-06 guidelines [7] as well as previous pull-out test studies [4,5].

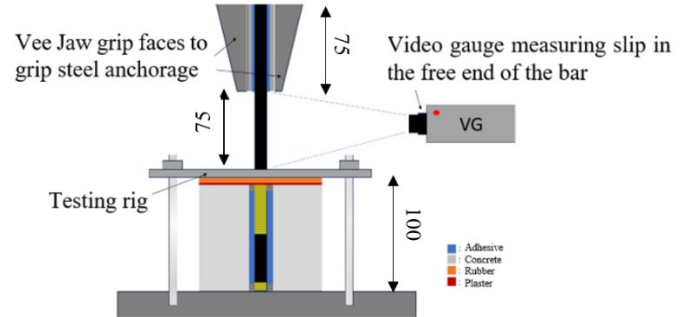


Fig. 2: Pull-out test setup.

The GFRP bars were cut into 250 mm lengths to ensure that the test specimens fit properly within the testing machine. A displacement controlled Instron testing machine was used to apply the pull-out force at a rate of 0.01 mm/s, with a maximum load capacity of 600kN. A thin layer of casting plaster of 5mm in thickness was used to provide a flat surface at the concrete portion. The specimens were then bound in place using a 15 mm thick, steel plate placed across the top of the plaster. The plate was fixed in place using M20 high tensile steel bolts, while the loading on the bar was increased gradually. The plaster ensured uniform contact with the restraining plates.

To ensure that the GFRP bar remained undamaged during testing, a 75mm long hollow steel tube with 20mm external diameter and 4mm wall thickness was bonded to the upper end of the FRP bar using the Araldite 2019 epoxy resin. The steel tube surrounding the FRP bar was then gripped by the testing machine. The length and width of the anchorage was designed in accordance to ACI 440.1R-06 specifications [7].

The pull-out force exerted on each sample was recorded internally using an automated data acquisition system, using the software on the Instron machine. A video gauge was placed in front of the visible section of the GFRP bar, recording the slip (displacement) at five equally spaced points (10mm separation) in the bar. The effect of the extension was accounted for, generating five slip values at peak pull-out force. An average was taken of these to give the final maximum slip value.

### 3. Experimental Results

This section provides a comprehensive analysis of the pull-out test results which are presented in terms of pull-out force and average bond stress-slip relationships. The effect of concrete type and strength, GFRP bar diameter and hole diameter on the pull-out force and bond stress are explained. Table 1 gives the peak pull-out force, maximum average bond stress, slip at peak pull-out force and failure mode for each tested specimen.

The correlation between the average bond stress ( $\tau$ ) and pull-out force ( $P$ ) is expressed by ACI 440.1R-06 [7] as in Eq.(1):

$$\tau = \frac{P}{\pi d_b l_b} \quad (1)$$

where  $l_b$  is the embedded length of the bar and  $d_b$  is the bar diameter.

Eq.(1) assumes the average bond stress to be constant along the embedded length. This assumption allows comparison of the average bond stress-slip curves.

All samples followed the same failure mode of bar pull-out (slip) at the adhesive/concrete interface without developing cracks on the concrete surface. This was expected, confirming previous findings [4,5], due to the low embedded length values ( $5d_b$ ) of the specimens.

Three sets of specimens were tested twice to ensure repeatability of the results. The duplicate sets of specimens: (i) LC22-GFRP10- $5d_b$ - $1.8d_b$  and (ii) LC22-GFRP10- $5d_b$ - $1.5d_b$  had a difference in pull-out force at failure of 2.03 kN (19.3%) and

1.06 kN (12.9%), respectively. Whereas, the corresponding difference in the maximum average bond stress was 0.18 MPa (4.2%) and 0.86 MPa (34.6%), for sets (i) and (ii), respectively. The third set of specimens, C22-GFRP12-5db-1.5db, had a difference in peak pull-out force and maximum average stress of 3.69 kN (40.8%) and 0.85 MPa (31.2%), respectively. The variation observed between repeated specimens could be related to bubble formations within the adhesive that form during application, which can reduce the strength of the adhesive/concrete interface.

### 3.1. Stiffness of Bond-Slip Curves

Fig. 3a and b illustrate the pull-out force-slip and average bond stress-slip curves for the specimens with 10 mm GFRP bars, respectively. The corresponding curves for the specimens with 12 mm GFRP bars are illustrated in Fig. 4a and b, respectively.

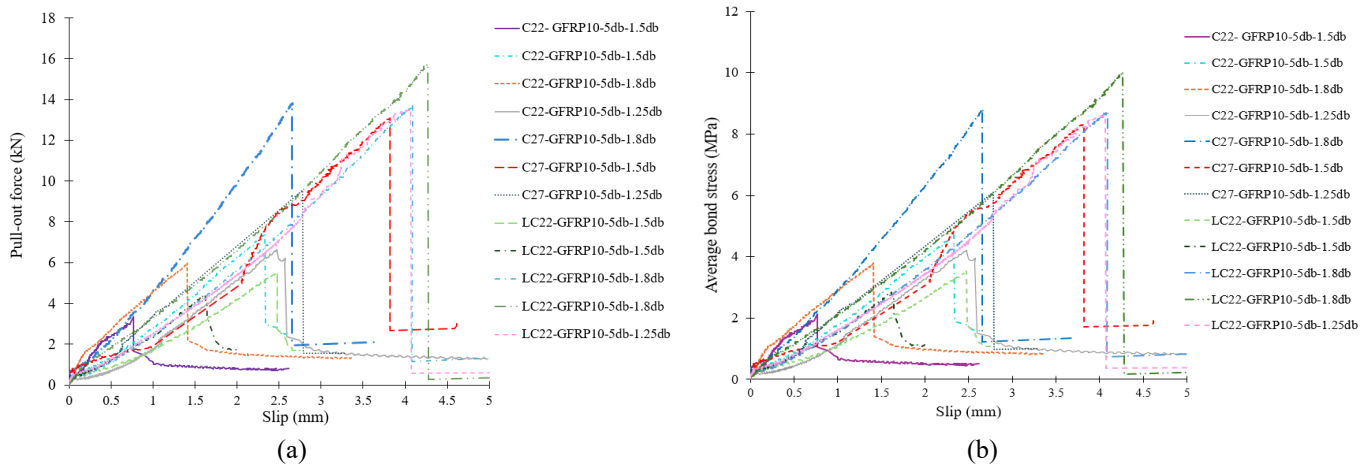


Fig. 3: Bond-slip curves for the specimens with 10 mm GFRP bars: (a) pull-out force-slip curves and (b) average bond stress-slip curves.

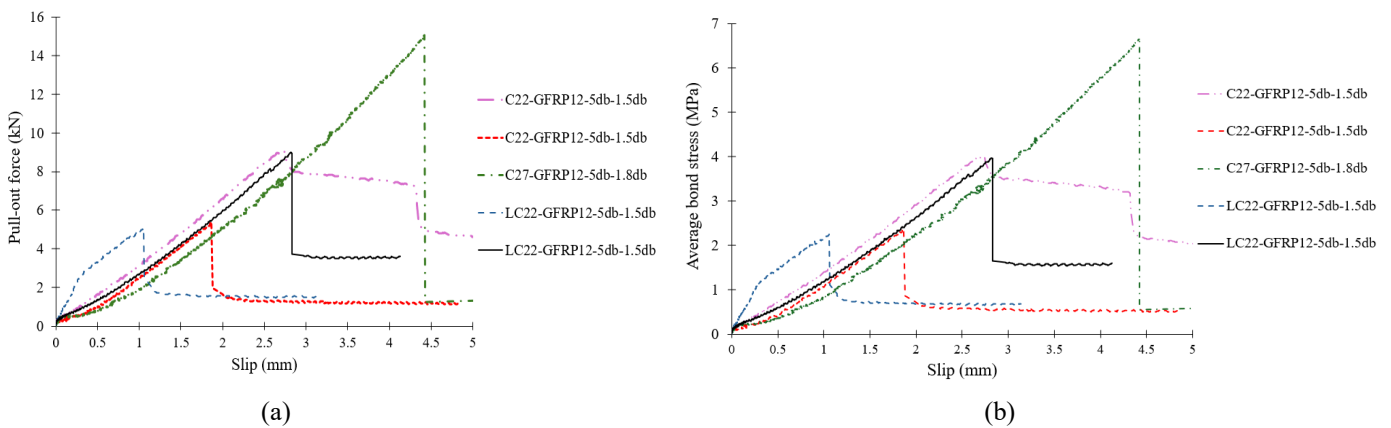


Fig. 4: Bond-slip curves for the specimens with 12 mm GFRP bars: (a) pull-out force-slip curves and (b) average bond stress-slip curves.

The global bond behaviour of these curves is characterised by an initial, almost linear, increase in the pull-out force (or average bond stress) with slip (ascending branch), followed by a descending branch once the maximum pull-out force (or average bond stress) has been achieved. Of note, pull-out force-slip curves evaluate the bond behaviour along the whole contact surface, rather than on a localised level. The values can be considered as a summation of the localised bond stresses and resulting slips at points along the bar [5]. As seen in Fig. 3a and b, the majority of OPC specimens had comparable initial

stiffness (i.e. the stiffness of the ascending branch), with exception to C27-GFRP10-5d<sub>b</sub>-1.8d<sub>b</sub>, which had a higher initial stiffness. The higher stiffness for this specimen was to be expected due to higher concrete compressive strength, which increases the resistance of the FRP-to-concrete interface [5]. The specimens with low carbon, AAC (LC22) displayed similar initial stiffness to the corresponding specimens of OPC with similar concrete compressive strength (C22), but obtained higher slip values corresponding to the maximum average bond stresses and pull-out forces (Fig. 3a and b). As the hole diameter increased from 1.25d<sub>b</sub> to 1.8d<sub>b</sub>, the initial stiffness of the pull-out force-slip (or average bond stress-slip) curves for the specimens with OPC (C22, C27) increased. As a result, the slip values corresponding to the peak pull-out forces and average bond stresses were lower for specimens with OPC (C22, C27) and a hole diameter of 1.8d<sub>b</sub>.

### 3.2. Effect of Bar Diameter

The impact of bar diameter on pull-out capacity and average bond stress was studied by comparing two sets of specimens: (i) C22-GFRP10-5d<sub>b</sub>-1.5d<sub>b</sub> and C22-GFRP12-5d<sub>b</sub>-1.5d<sub>b</sub>, and (ii) C27-GFRP10-5d<sub>b</sub>-1.8d<sub>b</sub> and C27-GFRP12-5d<sub>b</sub>-1.8d<sub>b</sub> (Table 1). The increase in bar diameter from 10 mm to 12 mm, resulted in a 1.6 kN (21.5%) and 1.2 kN (9.1%) increase in the pull-out capacity for the set of specimens (i) and (ii), respectively. Therefore, for a larger bar diameter, the greater bond area results in a higher pull-out capacity [5]. Whereas, the maximum average bond stress decreased by 0.7 MPa (18.2%) and 2.1 MPa (31.9%) for the corresponding set of specimens (i) and (ii), respectively. This decrease can be attributed to the higher amount of elastic energy available when using large diameter bars [4] and is also in agreement with the findings of other experimental studies who tested deep embedment GFRP bars epoxy-bonded into concrete specimens [5]. In addition, specimens with larger bar diameter also experienced greater slip values at peak pull-out force.

### 3.3. Effect of Hole Diameter

The impact of hole diameter (quantity of adhesive) on the bond behaviour was investigated by considering three specimens with different hole diameters: C22-GFRP10-5d<sub>b</sub>-1.25d<sub>b</sub>, C22-GFRP10-5d<sub>b</sub>-1.5d<sub>b</sub> and C22-GFRP10-5d<sub>b</sub>-1.8d<sub>b</sub>. Increasing the hole diameter from 1.25d<sub>b</sub> (12.5mm) to 1.5d<sub>b</sub> (15 mm) increased the pull-out capacity by 0.8 kN (12.2%), whereas the further increase in hole diameter to 1.8d<sub>b</sub> decreased the pull-out capacity by 1.5 kN (24.8%). Similarly, increasing the hole diameter from 1.25d<sub>b</sub> (12.5mm) to 1.5d<sub>b</sub> (15 mm) resulted in a 0.51 MPa (12%) increase in the bond stress, whereas the further increase in hole diameter to 1.8d<sub>b</sub> decreased the bond stress by 0.96 MPa (25.4%). In addition, similar observation can be inferred by two more specimens of low carbon, AAC with two different hole diameters: LC 22-GFRP12-5d<sub>b</sub>-1.5d<sub>b</sub> and LC 22-GFRP12-5d<sub>b</sub>-1.8d<sub>b</sub>. As the hole diameter increased from 1.5d<sub>b</sub> (18 mm) to 1.8d<sub>b</sub> (22 mm), the bond stress decreased by 0.4 MPa (21.5%). This observation agrees with the test results of research study conducted by [4] who investigated the impact of the quantity of adhesive on the bond performance by considering three different hole diameters (1.25d<sub>b</sub>, 1.5d<sub>b</sub> and 2.0d<sub>b</sub>). It was concluded that as the hole diameter increased from 1.25d<sub>b</sub> to 1.5d<sub>b</sub>, the bond performance was improved leading to better confinement and greater bond stress. In contrast, such behaviour was not exhibited for larger holes sizes ranging from 1.5d<sub>b</sub> to 2.0d<sub>b</sub> where the bond stress was reduced. The effect of confinement was reduced as a result of possible greater shrinkage that occurs in larger holes compared to smaller ones [4,5].

### 3.3. Effect of Concrete Type and Concrete Compressive Strength

The effect of concrete compressive strength on pull-out capacity and maximum average bond stress can be inferred from specimens C22-GFRP10-5d<sub>b</sub>-1.5d<sub>b</sub> and C27-GFRP10-5d<sub>b</sub>-1.5d<sub>b</sub> (Table 1). As the concrete strength increased from 21.6 to 26.5 MPa, the pull-out capacity increased by 5.7 kN (75.8%). C22-GFRP10-5d<sub>b</sub>-1.5d<sub>b</sub> and C27-GFRP10-5d<sub>b</sub>-1.5d<sub>b</sub> had the same embedment length and bar diameter and thus the maximum average bond stress increased by 3.6 MPa (75.9%) due to the increase in concrete compressive strength. This observation supports previous findings made by [5] who reported that increasing the concrete strength from 26.1 to 45.6 MPa, resulted in a 18.6 kN (33%) increase in pull-out capacity. It can be suggested that increasing the concrete compressive strength increases the resistance of the FRP-to-concrete interface, which enhances the bond strength.

This study investigated, for the first time, the effect of concrete type on pull-out capacity and maximum average bond stress by comparing two specimens LC22-GFRP10-5d<sub>b</sub>-1.8d<sub>b</sub> and C22-GFRP10-5d<sub>b</sub>-1.8d<sub>b</sub> (Table 1). Both specimens had

the same embedment length, bar diameter, hole diameter and similar concrete compressive strengths. Results show that the pull-out force values were 15.73 kN for specimen with low carbon, AAC (LC22-GFRP10-5d<sub>b</sub>-1.8d<sub>b</sub>) and 5.97 kN for the corresponding specimen with OPC (C22-GFRP10-5d<sub>b</sub>-1.8d<sub>b</sub>). Thus, the pull-out force of specimen with low carbon, AAC is 2.6 times that of specimen with OPC. In addition, the bond stress for the AAC specimen (LC22-GFRP10-5d<sub>b</sub>-1.8d<sub>b</sub>) was about 6.2 MPa greater than the corresponding value for the specimen with OPC (C22-GFRP10-5d<sub>b</sub>-1.8d), confirming a better bond performance.

It can be also observed that the specimen with low carbon, AAC (LC22-GFRP10-5d<sub>b</sub>-1.8d<sub>b</sub>) managed to reach a pull-out force of 1.92 kN (13.9%) greater than the specimen with OPC (C27-GFRP10-5d<sub>b</sub>-1.8d<sub>b</sub>) despite the latter having a concrete compressive strength 22.7% greater than the AAC specimen. Therefore, the results of this study show that specimen with low carbon, AAC had generally higher pull-out force and bond strength values, leading to a better bond performance than the corresponding specimens with OPC. It should be noted that DE technique relies on the chemical bond within the FRP-epoxy-concrete interface. It is plausible that the greater yield in pull-out force, and hence bond strength, is a result of a stronger chemical bond due to the different chemical composition of the low carbon, AAC binder in comparison to OPC. It can be suggested that AAC binder may contain similar polar molecular groups that are mutually attractive and chemically compatible to the adhesive and FRP rod which can enhance the shear transfer in the FRP-epoxy-concrete interface.

#### 4. Conclusions

This research study investigated, for the first time, the bond performance of DE GFRP bars epoxy-bonded into a new type of low carbon, AAC which was tested against Ordinary Portland cement (OPC). The impact of concrete type, concrete compressive strength, GFRP bar diameter and hole diameter on the bond strength was examined. Based on the results of this study, the following conclusions can be made:

For the specimens with DE GFRP bars, the pull-out capacity increased with the increase in bar diameter and concrete compressive strength. The bond strength reduced when larger diameter (i.e. 12 mm) GFRP bars were used. The average bond stress was greater for smaller diameter (i.e. 10 mm) bars, confirming an inversely proportional relationship between the bar diameter and the bond stress. The specimens with low carbon, AAC achieved higher pull-out capacity and better bond performance than the corresponding specimens with OPC. The increase in hole diameter affected both the initial stiffness and failure loads of the specimens with DE GFRP bars. The results suggest that adopting a hole diameter of 1.5d<sub>b</sub> enhances the bond behaviour of the DE technique.

#### References

- [1] F. Althoey, W.S. Ansari, M. Sufian and A.F. Deifalla, "Advancements in low-carbon concrete as a construction material for the sustainable built environment." *D. Built. Envir.*, vol.16, no.100284, 2023.
- [2] O. Chaallal, A. Mofidi, B. Benmokrane, and K. Neale, "Embedded through-section FRP rod method for shear strengthening of RC beams: Performance and comparison with existing techniques." *J. Compos. Constr.*, vol.15, no.3, pp.374–383, 2011.
- [3] P. Valerio, T. J. Ibell, and A. P. Darby, "Deep embedment of FRP for concrete shear strengthening." *Proc. Inst. Civ. Eng. Struct. Build.* vol.162, no.5: pp. 311–321, 2009.
- [4] A. Godat, A. L'Hady, O. Chaallal, and K.W. Neale. "Bond behavior of the ETS FRP bar shear-strengthening method". *ASCE J. Compos. Constr.* vol.16, no.5:pp.529–539, 2012.
- [5] M. Caro, Y. Jemaa, S. Dirar, and A. Quinn, "Bond performance of deep embedment FRP bars epoxy-bonded into concrete." *Eng. Struct.* vol.147: pp.448–457, 2017.
- [6] M. Caro, S. Dirar, A. Quinn, and H. Yapa. "Shear strengthening of existing reinforced concrete beams with embedded bars - An overview". *Proc. Inst. Civ. Eng. Struct. Build.* vol.176, no.6: pp.439-452, 2021.
- [7] ACI (American Concrete Institute). Guide for the design and construction of structural concrete reinforced with FRP bars. Report No. 440 1R–06, Farmington Hills, MI, 44pp. 2006.
- [8] D.C. Teychenné, R.E. Franklin, and H.C. Erntroy. *Design of normal concrete mixes*. Garston, Watford, WD2 7JR, United Kingdom: Building Research Establishment Ltd, 1997.